The manuscript changes resulting from referee comments are highlighted and commented with the corresponding numbers in the manuscript below. The page and line numbers of the changes also correspond to the manuscript below.

All uncommented changes in the manuscript below are minor language corretions.

RC1 by Peter Greaves:

Referee comment:
I think this is a very interesting piece of work - I tried something similar to this during my PhD, but using much less robust methods. I found that the masses which were required seemed very high to me at the time, but I didn't appreciate that there are methods of applying these virtual masses which do not require them to be at the same height as the blade. This test method has the advantage over the test optimisation method being pursued by ourselves and others (in which the frequencies do not need to coincide) that much less information sharing needs to take place between test house and customer, but perhaps at the expense of a more challenging test set-up process.

Author response:
Thank you for the appreciative comments.

Referee comment:
I think it is very important that you validated your results with a nonlinear time-stepping simulation as the nonlinearities could lead to significant angular changes of the push rods.

Author response:
A nonlinear time-stepping simulation has been performed as mentioned on page 7 line 9-11 and page 10 line 3-5. The angular changes of the pushrods occurred, but did not significantly change the results compared to the harmonic simulation. The angular changes also depend significantly on the length of the pushrods. The longer the pushrods, the smaller the angular changes. At outboard positions with high deflections the pushrods would need to be unreasonably long to prevent high angular changes. Hence, at the most outboard positions no load elements requiring pushrods were allowed in the test desing.

Corresponding change #1: Page 7 lines 21-26

Referee comment:
For the iteration to obtain the aerodynamic loads, I have considered a different way of doing this which may be of interest: 1 - Scale the mode shape so that the test loads match the target loads in a least squared sense 2 - Calculate energy dissipated during cycle by aerodynamic and structural damping (using a damping matrix generated by Rayleigh method) 3 - Use the actuator displacement to calculate the actuator force by equating the energy in (integral of actuator force x distance over cycle) to the energy out (air resistance and structural damping)

Author response:
Interesting method, but as I understand this only helps to predict the required actuator force. The effect of aerodynamic damping on the load distribution cannot be predicted, which was the goal in the present work.

Referee comment:
If it is possible, it would be very interesting to know a rough size range for the blade (I appreciate you can't share the exact length as this can identify the blade) as this would help contextualize the magnitude of the loads and masses required.

Author response:
The Blade is more than 60m long. For Information cannot be provided.

Corresponding change #2: Page 9 line 16

Referee comment:
Overall, congratulations on a great piece of work!

Author response:
Thank you for your helpful comments!

RC2 by Nathan Post:

General comment:

Referee comment:
This paper summarizes some key aspects of performing resonance fatigue tests of large wind turbine blades and the challenges faced when considering biaxial testing of these blades. The new work presented in the paper is applying a 3-dimensional harmonic model to evaluating and designing a fatigue test. However, the information disclosed regarding the implementation of the model is insufficient to enable another researcher to implement this approach directly. It is discussed that scaling the deflection mode shape is performed but not clear how this is accomplished in the biaxial case.

Author response:
The mode shapes are not scaled, but the displacement excitation of the harmonic simulation. The harmonic simulation for biaxial testing is also not necessarily exciting at a natural frequency of the system.

The deflection is realised by displacement excitation using two actuators. The biaxial simulation is scaled iteratively. First a small displacement is applied in both actuators at the same time using a phase difference as described on page 5. After evaluating the load distribution two scaling factors for the flapwise and lead-lag load are computed. These are multiplied with the corresponding blade deflection at excitation position. The actuator stroke for the next simulation is then computed using eq. (1) and eq. (2). This scaling procedure is repeated until convergence.

Corresponding change #3: Page 7 lines 10-18

Referee comment:
Also, the tendency of a typical blade to not have perpendicular movement in the flap and lead-lag directions due to the twist and relative frequencies is not addressed. While the actuators might be placed at angles, the blade motion might also be at an angle.

Author response:
This tendency of the blade is rather key element of the load element procedure. This is mentioned on page 4 line 18: "as a rotor blade oscillates in one of its first mode shapes, the direction of displacement is not necessarily aligned with the main directions of the blade..." The not-perpendicular movement is also displayed in Figure 2(a).

Corresponding change #4: Page 4 lines 24-26

Referee comment:
Finally, no mention of incorporating the bend twist coupling in the model is addressed.

Author response:
The bend twist coupling is not mentioned specifically, but the general coupling of different degrees of freedom (if applicable) is taken into account in the simulations as described in section 2.1.

Corresponding change #5: Page 4 line 9

Referee comment:
So, they have added complexity to the model while not demonstrating the superiority or even the difference between this approach when compared to performing the 2 simultaneous 2D harmonic models employed by Post et al. (Post 2016).

Author response:
By performing two simultaneous 2D simulations as employed by Post et al. (2016) the flapwise and lead-lag loading can be evaluated independently very well. But when considering coupled mode shapes, load introduction elements with tilted angles of inclination, and multiple non-perpendicular excitations at different phase angles only 3D simulations are applicable. Since the goal of this work was to incorporate all of these effects the superposition of 2 simultaneous 2D simulations would not suffice.

Corresponding change #6: Page 3 lines 15-16

Referee comment:
The use of spring elements is suggested – however, it is not obvious how such springs could be implemented effectively on a test since in this application they are subjected to reversing load cycles and most typical long displacement springs are either compression or tension, not both. Also withstanding the number of load cycles could be difficult.

Author response:
Since the current work is a numeric study, tension-compression-spring elements were used in the simulation. How these springs are to be realized in reality is not part of this work. However, this aspect is under investigation and such information will be available in the near future.

Referee comment:
There is a brief discussion of the actuator displacements in a skew coordinate system which the reader assumes is used in the simulation (are they taken as displacement actuators rather than force actuators in the simulation?). It is not clear if the controls in the simulation assume contribution of each actuator in each direction. Since the change in angles of the actuators with displacement is neglected in the model it isn't clear what information is gained in this part of the analysis rather than just setting up the actuators to be perpendicular in the test.

Author response:
Yes, the excitation is implemented displacement driven. Since the actuators are not perpendicular and at angles both actuators contribute to both directions.

Corresponding change #7: Page 5 line 16-17 Page 6 line 1

Referee comment:
Validation of the results was not conducted experimentally, nor were the results compared to previous simulation approaches in a rigorous way.

Author response:
The uniaxial simulation procedure was validated using confidential data of different blades. Experimental results for validation of biaxial simulations are not available at this stage. The comparison to previous biaxial simulation approaches is hardly possible since no published approaches consider 3D-motion and fully populated stiffness matrices.

Also further comparisons to experiments and other simulations would go beyond the scope of this work.

Referee comment:
A note that the resulting moments are within 3

Author response:

I believe there is a part of the comment missing

Specific comments:

Referee comment:
Page 3, 1 – 10. Reference is made to spring elements in the context of Post 2016. However, that report does not discuss the use of spring elements and instead uses the concept of negative virtual masses created with a hydraulic actuator to “remove” or carry mass from the blade and load frames. While the effect is similar in that both a spring or a negative virtual mass provide a force in the opposing and proportional to the displacement (and the equivalent spring constant k=-mA(2pi f)^2 a virtual mass with negative value of m with displacement amplitude A and frequency f) this is not a discussion that is included in Post 2016. In that report the authors discuss using actuators to remove the effect of mass thus introduction negative virtual masses into the test design. Recommend rewriting these paragraphs to accurately paraphrase the Post 2016 report and then introduce the concept of springs and the associated math separately.

Author response:
Thank you for clarifying. This is changed accordingly:

Corresponding change #8: Page 3 line 4-12

Referee comment:
Page 4, lines 19-24. This part of the paragraph doesn’t make sense to me and I am not sure what the authors are trying to convey. How does the blade oscillate in different directions?

Are we talking about for a uniaxial test or a biaxial test?

The sentence “The effect of an element on the eigenfrequency, which is not to be affected, shall be minimized.” makes no sense to me. Each element of the blade or saddle, mass, virtual mass or spring will change the eigenfrequency. Also, it isn’t clear how this leads to the following sentence that the elements (which elements? load elements?) must be perpendicular to the mode shape of the blade. And what is not to be affected? I take it that you are trying to say that the load element vectors should be perpendicular to the local movement of the blade in the other mode-shape so as not to impart energy in that direction? I think that this relationship might influence the phase angle of the test and relative amplitude of the directions, but it is unclear how it would significantly impact the frequency or mode shape.

Author response:
Not the blade oscillates in different direction but the oscillation direction changes slightly along the blade. Hence, the motion near the root has a slightly different direction than the motion at the tip.

We are talking about general mode shapes of the blade, not about testing.

Since the first flapwise and first lead-lag mode shapes are not perpendicular, the load element direction needs to be defined more specifically. In order to affect mainly the first flapwise frequency by a flapwise load element and only in a negligible amount the first lead-lag frequency, the element is oriented perpendicular to the corresponding lead-lag mode shape direction, rather than in line with the flapwise mode shape direction. Vice versa for a lead-lag load element.

Corresponding change #9: Page 4 line 22-24
Also, see Changes #3 Page 7 lines 10-18

Referee comment:
Also, the actuators will be of finite lengths so the angles will change throughout the test and thus will impart some virtual mass effect in the perpendicular direction.

Author response:
This is true, but using the described procedure of orienting the load elements this effect is reduced to a minimum

Referee comment:
Finally, the skew of the actuators discussed on page 5 seems to go counter to the argument made here.

Author response:
The actuators are supposed to excite the test and not affect the natural frequencies. Due to the applied springs

and virtual masses the mode shapes of the total test setup differ from the mode shapes of the blade. In order to excite the test in these new mode shapes the actuators are applied accordingly.

Referee comment:
Page 5, line 7 and 8. The authors state "The phase angle needs to be controlled during the test therefore, the hydraulic actuators need to be attached at the same position along the blade length". What is the reason for this? It is not clear to this reviewer that this statement is true. While you do need to control the phase angle, this is controlled with the relative phase of the excitation of each actuator. The blade will move in its mode shape and phase angle regardless of where each exciter is placed along the blade length.

Author response:
The phase between the flapwise and lead-lag motion depends purely on the phase between the actuator displacements. When placing the actuators at the same position the phase of flapwise and lead-lag motion at this position directly corresponds to the actuator phase. When placing the actuators at different positions instead, it is harder to control the phase angle of the blade. This would require a complex controller, since the phase of motion at different cross section varies and depends on the mass and stiffness distribution. Using the same phase of excitation at different positions would result in different blade movements.

Corresponding change #10: Page 5 line 10-15

Referee comment:
Page 6, line 2-3. Neglecting the non-linear displacement seems like a large oversight given the 3D model. Are the actuators force or displacement actuators? Depending on how significant the angles are and recognizing that for an elliptical test with a 90 deg phase angle, the maximum force of the actuator occurs at maximum angle it seems like this could be a significant loss in test efficiency and thus greater than simulated forces would be required in reality to run the test. Suggest expanding this discussion and better highlighting the impacts of the assumptions made and how the forces are introduced in the simulation.

Author response:
They are displacement actuators. Since harmonic simulations do not permit nonlinearities, neglecting them is inevitable. Though, this fast simulation method is only used to compare different test setups with each other in the design process. For this purpose mainly qualitative comparison is necessary. Hence, the harmonic simulation is still valid. When evaluating the final setup non-linear transient simulations are utilized to confirm the results.

Corresponding change #11: Page 6 line 8-9

Referee comment:
Page 6, line 29-30: For a biaxial test, isn't the objective to modify the flap and lead-lag frequencies to be the same (1:1 test) so it isn't clear why they are different to start with. Do you mean that you are taking the mean of the uniaxial test cases as the guess for starting the biaxial test case?

Author response:
The two different frequencies are natural frequencies of the system, which are derived from the preceding modal analysis. The objective is to modify these natural frequencies to be the same or at lest close to each other. But in order to find such a test setup different setups need to be evaluated. Hence, the simulation uses a single forced excitation frequency which is between these natural frequencies.

Corresponding change #12: Page 7 line 8-9

Referee comment:
Page 7, lines 4-8: While the iteration on the damping is included it isn't clear how this process adjusts the masses and springs to achieve the same frequency in both mode shapes for the biaxial test. At some point you are optimizing for maximum frequency within the bending moment limits but again it isn't clear how this is performed for the biaxial test while keeping the frequency in the flap and lead-lag directions the same. A flow

chart or itemized list of steps of the simulation and optimization process would be helpful to clarify when each step is performed and what the objective functions are for each step.

Author response:
The simulation procedure itself does not adjust the masses and springs. To achieve the same frequency the optimization described on page 8 is used to adjust these values.

The suggested flowchart is added to the work.

Corresponding change #13: Page 7 line 3 Page 8 line 16 – page 9 line 2
Additional figure 4: Page 8 lines 5-7 (all following figures are raised in number)

Referee comment:
Page 7, lines 10-11: As mentioned previously this comparison of the model results to the transient test (and how the transient test was constructed) would be good to include here (or later when comparing results in which case don't mention it hear but do describe the other simulations that you compare the results to. Also a comparison to a simpler 2D harmonic approach would be very interesting as well and make this a stronger paper.

Author response:
The detailed description of the transient simulation as well as comparison to other simulation approaches would go beyond the scope of this work. They are reserved for future work.

Referee comment:
Page 8, line 17: spring elements are assumed to be massless? It is unclear how this would be accomplished. At a minimum a load frame is required to introduce the load to the blade from the spring and real springs do have mass so this seems like a gross oversimplification when designing the test.

Author response:
When designing the spring elements in reality their stiffness would be chosen in such a way, that its own mass is compensated and the "active" stiffness delivered to the blade would be equal to the stiffness in the present case. This way the assumption of "massless" springs is valid.

Referee comment:
Page 13 line 2: Allowing higher overloads outside of test regions is definitely something that would need to be taken on with care. Maybe if there is significantly more safety factor in that region of the blade it would be ok but it would be surprising if this is in generally reasonable. Same with reinforcing the blade in those regions – which will be difficult to do without creating stress concentrations.

Author response:
The arguments in this comment are adopted accordingly

Corresponding change #14: Page 13 line 6-9

Referee comment:
Page 13, line 10. How did the optimizer end up exceeding one of the constraints? This needs to be explained since it should have found a solution within the constraints imposed, right? While this might be the "best" test solution for the blade, it isn't clear how the would have gone there without the user allowing it.

Author response:
The optimizer searches for the minimal value of the objective function, which consists of a sum of the actual objective and penalty values for constraint violations. If the algorithm is not able to find a design point which satisfies the constraints still the design point which gets the closest, while minimizing the actual objective, can be used as output of the optimization.

Technical corrections:

Referee comment:
Page 2, line 14: “In order to safely proceed testing : : :” should be “In order to safely proceed with testing”
Page 3, line 3: Reference (Post, 2016) is not included in the list of references at the end of the paper.
Page 5, line 18: “Angle of attack” isn’t a term that makes sense here since we generally think of that as an aerodynamic term. I think you mean the angle of incidence to the blade (or loadframe) – the alpha and beta in Figure 3. Suggest rewording this.

Author response:
The technical corrections are applied as suggested

A novel rotor blade fatigue test setup with elliptical biaxial resonant excitation

David Melcher[1], Moritz Bätge[1], Sebastian Neßlinger[2]

[1]~~Divison Structural Components~~ Department of Rotor Blades, Fraunhofer IWES, Fraunhofer Institute for Wind Energy Systems, Am Seedeich 45, 27572 Bremerhaven, Germany
[2]Nordex Energy GmbH, Langenhorner Chaussee 600, 22419 Hamburg, Germany

Correspondence to: David Melcher (david.melcher@iwes.fraunhofer.de)

Abstract. The full-scale fatigue test of rotor blades is an important and complex part of the development of new wind turbines. It is often done for certification according to the current IEC (2014) and DNV GL AS (2015) standards. Typically, a new blade design is tested by separate uniaxial fatigue tests in both main directions of the blade, i.e. flapwise and lead-lag. These tests are time consuming and rather expensive due to ~~a~~ the high number of ~~required~~ load cycles required, up to 5 million. Therefore, it is important to run the test as efficiently as possible. During fatigue testing, the rotor blade is excited at or near its resonant frequency. The trend for new rotor blade designs is toward longer blades, leading to a significant drop in their natural frequencies, and a corresponding increase in test time. ~~In order t~~To reduce the total test time, a novel test method aims to combine the two consecutive uniaxial fatigue tests into one biaxial test. The biaxial test excites the blade in both directions at the same time and at the same frequency, resulting in an elliptical deflection path of the blade axis. Using elliptical loading, the counting of damage equivalent load cycles is simplified in comparison to biaxial tests with multiple frequencies. In addition, the maximum loads in both main directions remain separated, while off axis loading is introduced. To achieve such a test, specific load elements need to be arranged so as to equalize the natural frequencies of the test setup for both test directions. This is accomplished by adding stiffness or inertial effects in a specific direction.

This work describes a new method to design suitable test setups. A parameterized finite element (FE) model of the test with beam elements for the blade represents the test setup. A harmonic analysis on the FE-model can identify the load distribution and the test conditions of a specific test setup within seconds. An optimization algorithm that varies parameters of the model and searches for the optimal setup is then applied to the analysis. This approach ~~enables~~ allows the efficient determination of a test setup, suited to the predefined requirements. The method is validated by ~~application~~ applying it to ~~on~~ three different test scenarios for a modern rotor blade: a) state-of-the-art uniaxial setups, b) uniaxial setups including springs and c) a biaxial setup. In conclusion, the resulting setups are evaluated in terms of test quality and efficiency.

1 Introduction

Rotor blades of wind turbines are exposed to very high fatigue loading over their ~~common~~ usual lifetime of 20 years in the field. Hence, their reliability and structural integrity are very important, from both an economic and a safety perspective. When a new rotor blade design is developed, it needs to be certified before it can go into operation. The design and certification of wind turbine rotor blades is ~~done~~ performed according to the current IEC (2014) and DNV GL AS (2015) standards. One essential part of the certification process is full-scale fatigue testing. These tests are performed to validate the calculations and assumptions made in the design models, by applying damage equivalent loads to the blade. Typically, two consecutive tests are done, in which the blade is separately loaded in the two main directions, i.e. flapwise and lead-lag. A drawback of these unidirectional tests is that the loads introduced into the blade do not necessarily represent the loading the blade will experience under field conditions, as Rosemeier et al. (2018) have shown.

The following requirements are considered in fatigue testing: ~~A~~ a target bending moment distribution, derived from the design requirements, needs to be matched or exceeded everywhere within the area of interest, while keeping the exceedance as small as possible in order to avoid unrealistic failures. If a section of the blade is overloaded, it can be damaged before the rest of the blade has been fully tested. In order to safely proceed with testing, ~~these~~ this damage~~s~~ needs to be repaired, which can lead to prolonged testing times. Besides the required load distribution, a high test ~~-~~frequency is desired to reduce the total testing time. The energy consumption of the test is another important boundary condition. Moreover, the introduction of high local shear forces to the blade should be avoided.

A state-of-the-art fatigue test setup involves the application of different load elements, i.e. actuators and masses, along the span of the blade, while the root of the rotor blade is attached to a test block. The actuators excite the blade at or near the corresponding system resonant frequency, while the masses are attached to the blade to tune the bending moment distribution. Forcing the blade to oscillate at a frequency significantly outside the resonant frequency leads to high shear forces at the load introduction and high energy ~~-~~consumption ~~of~~ by the test.

Attempts have been made to improve these uniaxial full-scale fatigue tests. Lee and Park (2016) for example used an algorithm to optimize the overloading by determining the optimal mass distribution, actuator position and excitation frequencies. Similarly, Zhang et al. (2018) evaluated a different optimization algorithm and included the position of the blade tip cut off as a design variable. Eder et al. (2017) proposed a uniaxial multi-frequency approach to replicate the actual spatial damage distribution of the blade more realistically.

Combining the two uniaxial tests into one biaxial test, which ~~implies~~ involves exciting the blade in both directions at the same time, is an approach to save testing time. It also has the potential to emulate the comprehensive damage along the blade's circumference (Heijdra et al., 2013). Exciting the blade at two different resonant frequencies, ~~resulting in~~ which equates to a random phase biaxial fatigue test, has ~~already~~ been ~~researched~~ the subject of research for a number of years (White, 2004; White et al., 2005; Greaves et al., 2012; Snowberg et al., 2014). Another approach for biaxial testing is ~~the~~ phase~~-~~-locked excitation, where the excitation frequencies in the flapwise and lead-lag directions have a specific ratio, e.g.

1:1 or 1:2 (White et al., 2011). Heijdra et al. (2013) proposed ~~to excite~~exciting the flapwise mode in its natural frequency while forcing the lead-lag motion in the same frequency to ~~get~~ obtain a 1:1 ratio. A method to achieve the desired frequency ratio while exciting both directions in resonance is to tune both natural frequencies independently ~~with~~ using the concept of virtual masses ~~and spring elements~~ (Post et al., 2016). These elements are connected to the blade in such a manner~~,~~ that they only add or subtract inertia ~~or stiffness~~ in one specific direction.

Kommentiert [MD1]: #8

This work focuses on the ~~phase~~ phase-locked resonant biaxial excitation with a frequency ratio of 1:1. ~~This way e~~Each cross section along the blade axis thus follows an ellipse, as depicted in Fig. 1(b). This simplifies the counting of damage equivalent load cycles when compared to biaxial tests with multiple different frequencies. ~~To tune~~ Virtual masses are used to adjust the natural frequencies so as to be equal or very close to each other, i.e. raising the flapwise and/or lowering the lead-lag natural frequency, ~~virtual masses~~ ~~and spring elements are used~~ as Post et al. (2016) suggested. Rather than using negative virtual masses to remove inertia from the system, our approach uses spring elements instead to add stiffness. Adding stiffness or removing inertia at a specific position has a similar physical effect on the natural frequencies of the system. ~~This~~ The result~~s~~ ~~in~~ is a test setup as ~~indicated~~ illustrated in Fig. 1(a). Unlike Post et al. (2016), who simulated the two test directions independently, this work aims to consider the coupling of the two directions. Instead of two separate two-dimensional simulations, one three-dimensional simulation is performed. It is thus possible to consider the coupling of multiple load and deflection directions. Here, the virtual masses and spring elements are not just applied in the global flapwise or lead-lag direction, but tilted around the blade axis as described below. The method elaborated in the following was developed to optimize these biaxial fatigue test setups. Thus, it is used to identify which load element needs to be placed where along the blade, in order to generate a fatigue test that satisfies all test requirements as efficiently as possible.

Kommentiert [MD2]: #8

Kommentiert [MD3]: #6

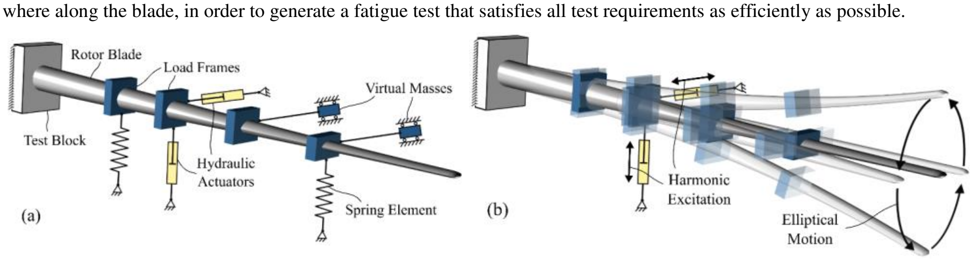

Figure 1: Biaxial fatigue test: (a) schematic of test setup, and (b) elliptical resonant excitation and resulting displacement.

2 Fatigue test simulation

To find a suitable test setup for either biaxial or uniaxial fatigue tests it is necessary to evaluate any given setup. A parameterized FE simulation tool was developed in ANSYS APDL to do so. Using specific design parameters, any desired test setup can be modelled with FE-elements. Moreover, ~~Subsequently~~ the ~~developed~~ tool runs various analyses (modal and harmonic) on the model to evaluate the properties of the given setup. This process is described in the following sub-sections.

2.1 Test setup modelling

The rotor blade is modelled using beam elements that are based on the Timoshenko beam theory. The properties of ~~those~~ these beam elements ~~consider~~ take into account coupling terms between different generalized strains and loads as they occur in composite structures. These properties, which are represented by mass matrices and fully populated 6x6 stiffness matrices, are derived from preceding analyses of multiple different cross sections along the blade.

The model of the blade is constrained at the root in all degrees of freedom to generate a cantilever beam setup. The loading elements, which are controlled by various parameters, are then attached to the beam elements as described below. Damper elements ~~are also attached in the model~~ representing the aerodynamic drag that occurs during testing are also attached in the model.

2.1.1 Loading elements

Masses attached to the blade ~~using~~ by means of load frames are applied directly to the beam model using point mass elements.

The load elements, which are designed to affect either the first flapwise or the first lead-lag frequency, can be virtual masses or spring elements. The virtual masses are modelled as mass elements that are connected to the beam elements using rigid body elements. They are constrained as shown in Fig. 2(a). The springs are modelled using linear spring elements.

These load elements must be attached in a specific direction; as a rotor blade oscillates in one of its first mode shapes, the direction of displacement is not necessarily aligned with the main directions of the blade. Additionally, the direction of a single mode shape ~~direction~~ changes along the length of the blade by a few degrees, meaning every cross section may oscillate in a slightly different direction. The first flapwise and lead-lag mode shape directions are not perpendicular to each other. The effect of ~~an element on the eigenfrequency, which is not to be affected,~~ a flapwise element on the lead-lag natural frequency and vice versa shall be minimized. Hence, it was found that the elements need to be attached so as to be perpendicular to the mode shape of the rotor blades, which is not to be affected. This is shown in Fig. 2(a) for one representative cross section, where a spring is applied in the flapwise direction and a virtual mass in the lead-lag direction.

The mode shapes of the test setup including springs and masses differ~~s~~ from those of the bare blade. As the hydraulic actuators are ~~supposed~~ intended to excite the test setup with the lowest possible energy consumption, they need to be

Kommentiert [MD4]: #5

Kommentiert [MD5]: #9

Kommentiert [MD6]: #4

attached in line with the direction of these new mode shapes. This is visualized for a biaxial test in Fig. 2(b). For a uniaxial test, only one cylinder is attached in the respective direction.

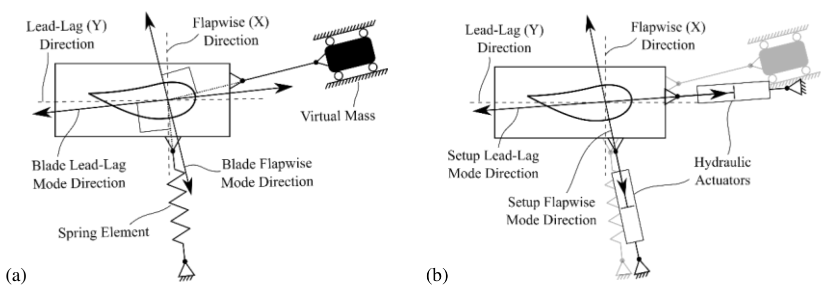

Figure 2: Angle for application of load elements: (a) passive elements according to blade mode shape, and (b) actuators according to setup mode shape.

For the biaxial test, the elliptical motion of the blade consists of two harmonic oscillations; one in the flapwise direction and one in the lead-lag direction, with a phase shift. This phase shift defines the tilt of the ellipse around the pitch axis and the width of the ellipse. With a phase shift of 90° the ellipse is not tilted, meaning the extreme loads in one main direction do not overlap with the extreme loads of the other direction, but rather with ~~its~~ their mean value. ~~The~~ This phase ~~angle~~ shift needs to be adjusted ~~controlled~~ during testing. ~~therefore, the~~ If both hydraulic actuators ~~need to be~~ are attached at the same position along the blade length, the phase shift between the flapwise and lead-lag motion is directly dependent on the actuator phase shift. Otherwise a complex controller system would be needed, since the phase of motion varies along the blade length and the phase shift would then also depend on the blade properties. Therefore, the actuators are kept at the same position in this work.

Kommentiert [MD7]: #10

As the hydraulic actuators may not be in line with the main directions of the blade and may not be perpendicular to each other, a skew coordinate system can be derived from their orientation as shown in Fig. 3.

Kommentiert [MD8]: #7

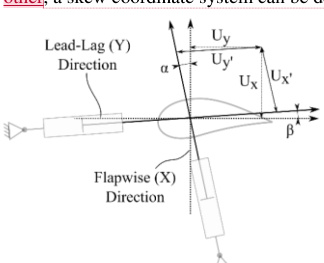

Figure 3: Blade coordinate system and skew coordinate system of actuators.

In order to find the correct displacement excitation for the actuators, the desired blade motion, including the phase ~~difference~~shift, must be converted to the skew coordinate system using Eq. (1) and Eq. (2).

Kommentiert [MD9]: #7

$$U_{x'} = U_x \frac{\cos\beta}{\cos(\alpha-\beta)} - U_y \frac{\sin\beta}{\cos(\alpha-\beta)} \tag{1}$$

$$U_{y'} = U_x \frac{\sin\alpha}{\cos(\alpha-\beta)} + U_y \frac{\cos\alpha}{\cos(\alpha-\beta)} \tag{2}$$

where U_x and U_y are the deflection values in the blade coordinate system and $U_{x'}$ and $U_{y'}$ the values in the actuator coordinate system. In the real test, the angle of ~~attack~~ incidence of the actuators will change constantly as the blade follows the elliptical motion. This ~~would~~ will result in a constantly changing skew coordinate system with moving origin. The longer the actuators are, the smaller the ~~angle~~ change in angle becomes. As ~~the~~ harmonic simulations ~~of the test does not~~cannot consider nonlinear ~~displacement~~ effects, this phenomenon has been omitted ~~from the simulation~~at this stage of the setup definition.

Kommentiert [MD10]: #11

2.1.2 Aerodynamic damping

The aerodynamic damping is modelled using linear damping elements. At each beam element of the blade, two dampers are applied~~;~~: one in the flapwise direction and one in the lead-lag direction. In the simulation, each damper applies a force to the blade~~,~~ which is proportional to the velocity in the corresponding direction.

The ~~Aerodynamic~~ aerodynamic drag force, which corresponds to the damping force, is nonlinear and can be computed using Eq. (3).

$$F_D = -\frac{1}{2}\rho A C_D |v| v \tag{3}$$

~~Where~~ where F_D is the drag force, ρ is the density of the air, A is the area perpendicular to the motion, C_D is the drag coefficient and v is the velocity.

To achieve the same energy dissipation with the linear damping elements as the aerodynamic drag would induce, the damping constant $C_{d,lin}$ for each element is adjusted accordingly. The theoretical formula for the energy due to aerodynamic drag within one cycle of harmonic oscillation, E_{drag}, is shown in Eq. (4). The formula for the energy of a linear damper, E_{damp}~~.~~, is given in Eq. (5). ~~When equating~~ Equating E_{drag} and E_{damp}~~,~~ allows the required damping constant ~~can~~ to be derived as shown in Eq. (6).

$$E_{drag} = \int_0^{1/f} F_D(t) v(t) dt = \frac{16}{3}\pi^2 f^2 \hat{u}^3 C_D \rho A \tag{4}$$

$$E_{damp} = 2\pi^2 f \hat{u}^2 C_{d,lin} \tag{5}$$

$$C_{d,lin} = \frac{8}{3} f \hat{u} C_D \rho A \tag{6}$$

~~Where~~ where f is the oscillation frequency and $\hat{u}$ is the displacement amplitude.

The drag coefficient C_D used in the simulation was taken from the investigations by Greaves (2018)~~. They~~, who derived a dependency for the drag coefficient of the displacement amplitude $\hat{u}$ and the aerofoil shape.

2.2 Simulation sequence

Once the test setup is modelled, including load elements and dampers, the simulation tool runs several consecutive analyses to evaluate the given setup. This sequence is summarized in Fig. 4. Since the damping constants depend on the test frequency and the displacement amplitude, ~~the damping constants are~~they initially set to zero, as ~~those~~ these variables are unknown at the beginning of the analysis. The first analysis is a modal analysis to find the natural frequencies of the test setup. The outputs are then used to find the excitation frequency for the test. For a uniaxial test, the natural frequency of the first mode in the corresponding direction is used directly ~~used~~ as the test frequency. For a biaxial test, the mean value between the first flapwise and the first lead-lag frequency is used as the forced excitation frequency. Hence, any given test setup can be evaluated regardless of the ratio between the natural frequencies.

The test is then simulated using a harmonic simulation with a~~n~~ small initial actuator ~~stroke~~ displacement as the excitation. The harmonic simulation is then evaluated and scaled by a specific factor. This scaling factor is calculated to ensure that the test bending moment within the entire area of interest matches, or is higher than, the target bending moment to meet test requirements. In the biaxial case, the excitations of both actuators are applied simultaneously. Separate scaling factors are hereby applied to the flapwise and lead-lag displacements, which are converted to actuator excitations using Eqs. (1) and (2) before repeating the harmonic simulation.

At this stage of the simulation, the test frequency and a preliminary displacement amplitude ~~is~~ are known. These are then used to update the damping constants of the damper elements; the harmonic analysis is then repeated. This iterative process of updating the damping and the scaled harmonic analysis is repeated until convergence is achieved. This concludes the simulation and the results of the last harmonic analysis are used to evaluate the given setup.

The major advantage of using harmonic analyses in the simulation process is the short processing time. It takes only a few seconds, enabling the computation of a multitude of different test setups. A transient simulation of the test, which ~~also~~ considers nonlinear damping and nonlinear geometric effects, such as angular changes of load introduction elements, ~~geometric and damping effects~~ requires ~~roughly~~ about 100 times more processing time. A comparison of transient and harmonic simulations yielded a difference of less than 3% ~~difference~~ in loading amplitudes within the area of interest. Hence, the harmonic results are sufficiently precise. Nevertheless, the final test setup needs to be checked by a transient simulation.

Kommentiert [MD11]: #13

Kommentiert [MD12]: #12

Kommentiert [MD13]: #3

Kommentiert [MD14]: #3

Kommentiert [MD15]: #3

Kommentiert [MD16]: #1

Kommentiert [MD17]: #1

3 Optimization

The process described in the ~~chapter~~ section above can be used to evaluate any given test setup. ~~In order to~~To find a suitable setup, different options need to be evaluated and compared. By varying the design parameters and evaluating the influence of these changes, an optimal test setup can be found using an optimization ~~-~~algorithm, as described ~~below~~in the following. This workflow is visualized in Fig. 4.

Kommentiert [MD18]: #13

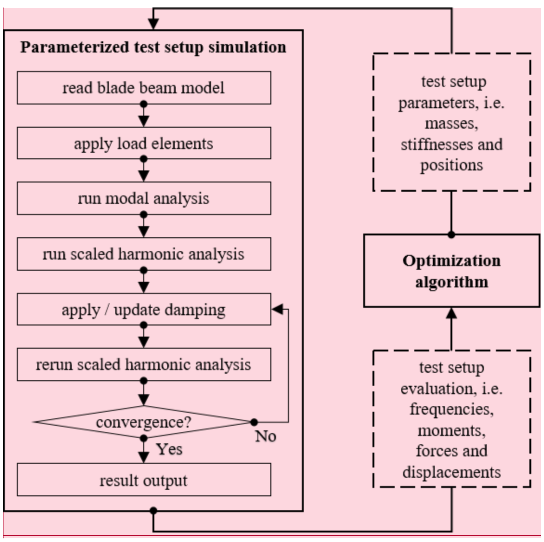

Figure 4: Flow chart of simulation sequence and optimization

Kommentiert [MD19]: #13

3.1 Problem formulation

The setups in this work are optimized to maximize the test frequency, i.e. shortest test time. This is done while keeping the ratio between test and target bending moment distribution within an allowable range. Within the area of interest the ratio must be above one to achieve the required load. To avoid overloading, an upper limit of 5% for flapwise and 10% for lead-lag loading was used. High local shear force introduction by the load elements needs to be avoided and the stroke amplitude of the actuator needs to be kept at a reasonable level. The design parameters that can be changed by the optimization are the mass or stiffness values of the load elements at specific defined positions along the blade. These can be attached in the flapwise or the lead-lag direction for the respective uniaxial test and in both directions for biaxial tests. Furthermore, the position of the actuators can be changed between the defined positions. For the optimization of the biaxial test, another constraint is introduced: In order for the excitation to be in resonance, the first flapwise and lead-lag natural frequencies need to be the same or close to each other. Hence, a limit of 5% deviation between the first flapwise and lead-lag natural frequencies is used.

Kommentiert [MD20]: #13

~~That~~ This leads to the problem formulation in Eq. (7), on which all the optimizations are based.

$$
\begin{aligned}
\text{Maximize:}\quad & \text{excitation frequency } f_{exc} \\
\text{With respect to:}\quad & \text{flapwise and/or lead lag mass or stiffness at each position} \\
& \text{actuator position} \\
\text{Subject to:}\quad & 1.00 \leq \frac{M_{x,Test}}{M_{x,Target}} \leq 1.05 \text{ within area of interest (biaxial and uniaxial flapwise)} \\
& 1.00 \leq \frac{M_{y,Test}}{M_{y,Target}} \leq 1.10 \text{ within area of interest (biaxial and uniaxial lead-lag)} \\
& 0.95 \leq \frac{f_{eig,flap}}{f_{eig,lead-lag}} \leq 1.05 \text{ (only for biaxial test)} \\
& F_A \leq 50 \text{ kN (for all load element forces)} \\
& u_A \leq 1 \text{ m}
\end{aligned}
\qquad (7)
$$

3.2 Boundary conditions

Further assumptions and boundary conditions are applied for the simulations and the optimizations; the load frames that are needed to connect the load elements to the blade, as well as the spring elements, are assumed to be without mass.

At each position, for each main direction, the optimization can use either a mass or a spring element. It is not possible to use both at the same position for the same direction, as they would simply cancel each other out.

If a parameter set defines virtual masses in both the flapwise and lead-lag directions at the same position, the smaller mass is attached directly to the blade as load frame mass, which acts in all directions. The larger mass is reduced to the difference between the previously defined masses, as this value still needs to act in one direction.

For the uniaxial setups, no virtual masses are allowed at all, as the natural frequencies of the blade do not need to be modified separately. Masses are instead applied as load frame masses. Springs for uniaxial testing are also only allowed in the respective test direction to raise the corresponding natural frequency.

3.3 Case study rotor blade

In this work, a modern industrial rotor blade more than 60m long is used to demonstrate the method developed ~~method~~[1]. The target bending moment distribution is given, and the area of interest is defined to be between 14% and 55% of the blade length. In this instance, the customer had previously defined the area of interest. Prior to testing, the blade tip was cut off at 90% of the blade length ~~in order~~ to reduce aerodynamic damping. The uniaxial tests are designed for 2.5 million load cycles in the flapwise direction and 5.0 million cycles in lead-lag direction~~, respectively~~.

Kommentiert [MD21]: #2

[1] Detailed information on the blade cannot be provided due to confidentiality constraints

As the biaxial test is performed elliptically, the same number of load cycles is required for both test directions. Therefore, the required number of load cycles for the biaxial test is defined as 5.0 million and the target load level for the flapwise direction is reduced to 94.25% of the uniaxial load level. This is done according to the international standard IEC-61400-23.

The possible positions for the load introduction are given in Table 1. These positions are defined in the test specification and thus are assumed to be appropriate for this purpose, and not to include critical regions of the blade. Other positions may contain critical areas, which need to be tested and must not be disturbed by load introduction equipment. Table 1 also contains the maximum spring element stiffness and the maximum mass at the corresponding position. These values are used to constrain the design space of the optimizations.

In the optimization for this blade, virtual masses or spring elements were only allowed up to the load position at 62% of the blade length. At 76% and 88% of the blade length, only load frame masses directly attached to the blade ~~have been~~were permitted. At these positions, the deflection of the blade is too high to reasonably consider virtual masses or spring elements.

Table 1: Load positions and boundary conditions for load element

Position [% of blade length]	26	38	48	62	76	88
Maximum stiffness [kN/m]	100	70	55	45	-	-
Maximum mass [t]	10.0	7.0	5.5	4.5	1.5	1.0

3.4 Case study optimizations

The method described ~~method~~ was used to generate three different test setups, including two state-of-the-art uniaxial setups for separate flapwise and lead-lag tests, which ~~are~~ were used as a baseline in the comparison. The uniaxial setups were then optimized again, allowing springs to accelerate the tests. Additionally, one biaxial setup was generated using springs and virtual masses. Finding a suitable biaxial setup was much more challenging for the optimizer in terms of computational effort, as there were more constraints to consider and more design parameters to change. The final setups generated by the optimizer were subsequently evaluated with nonlinear transient analyses, to check whether nonlinearities resulted in outcomes which were different ~~outcomes than~~ to those of the fast harmonic simulation. These ~~only~~ showed only minor differences for the given test setups.

4 Results

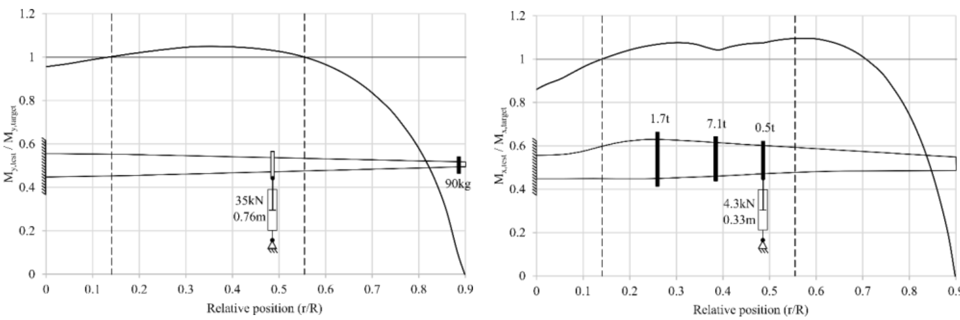

Figure 5~~4~~: Schematic of uniaxial test setups and test/target load ratio in flapwise (left) and lead-lag (right) directions

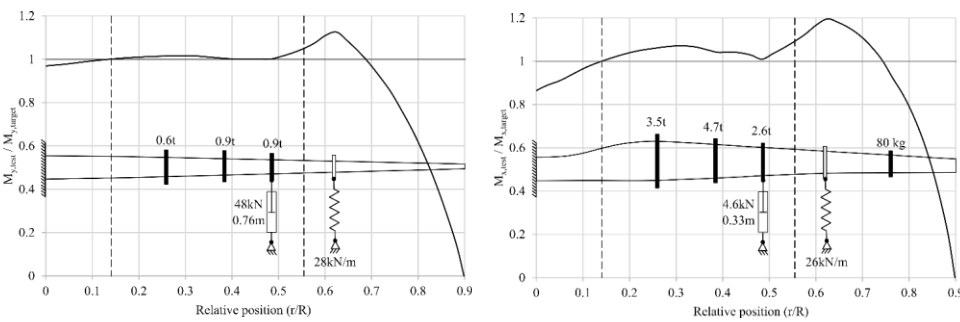

Figure 6~~5~~: Schematic of setups with springs and test/target load ratio in flapwise (left) and lead-lag (right) directions

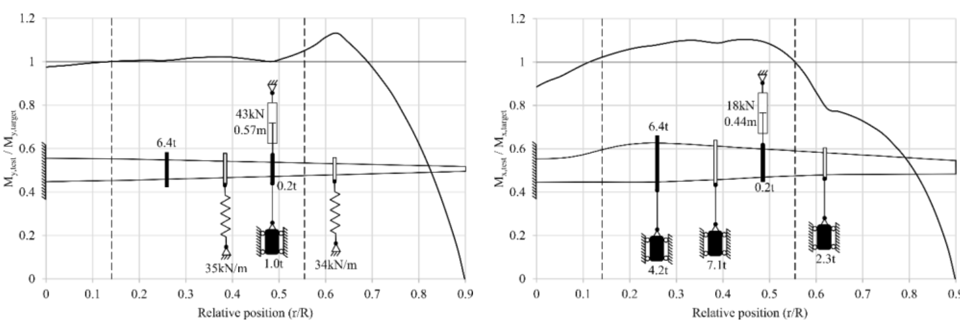

Figure 7~~6~~: Schematic of biaxial setup and test/target load ratio in flapwise (left) and lead-lag (right) directions

Figures ~~4~~ 5 to ~~6~~ 7 show the schematics of the setups that were found by the different optimization runs. In addition, the corresponding ratio between the actual moment distribution and the target distribution (flapwise direction: $M_{y,test}/M_{y,target}$; lead-lag direction: $M_{x,test}/M_{x,target}$) ~~over~~ plotted against the normalized position along the rotor blade (r/R) is shown. The borders of the area of interest are marked with dashed lines. Table 2 summarizes the ~~chosen~~ design parameters chosen and corresponding results of the ~~found~~ setups found. For all setups, the actuator was positioned at the third load frame at 48% of the blade length. This appears to be the position at which actuator force and stroke are balanced. Further outboard the stroke becomes too large, while further inboard the forces are too large, particularly in the flapwise direction. The optimizer used only ~~used~~ a ~~few~~ small number of springs ~~but~~ and otherwise favoured masses for the uniaxial setups, even when springs were permitted at the first four load frame positions. Additional springs would have a negative effect on the moment distribution.

Table 2: Summary of the optimized setups

Optimization results	Configuration		Uniaxial		Uniaxial (spring)		Biaxial	
	Direction		Flapwise	Lead-lag	Flapwise	Lead-lag	Flapwise	Lead-lag
Chosen design parameters	Actuator position		48%	48%	48%	48%	48%	
	Load frame mass [t]	at 26%	-	1.7	0.6	3.5	6.4	
		at 38%	-	7.1	0.9	4.7	-	
		at 48%	-	0.5	0.9	2.6	0.2	
		at 62%	-	-	-	-	-	
		at 76%	-	-	-	0.08	-	
		at 88%	0.09	-	-	-	-	
	Virtual mass [t]	at 26%	N/A	N/A	N/A	N/A	-	4.2
		at 38%	N/A	N/A	N/A	N/A	-	7.1
		at 48%	N/A	N/A	N/A	N/A	1.0	-
		at 62%	N/A	N/A	N/A	N/A	-	2.3
	Spring stiffness [kN/m]	at 26%	N/A	N/A	-	-	-	-
		at 38%	N/A	N/A	-	-	34.9	-
		at 48%	N/A	N/A	-	-	-	-
		at 62%	N/A	N/A	27.6	25.8	34.2	-
Target and constraint results	Frequency [Hz]		0.574	0.789	0.666	0.807	0.680	
	Test duration [days]		50.4	73.4	43.4	71.7	85.1	
	Actuator stroke [m]		0.76	0.33	0.76	0.33	0.57	0.44
	Actuator force amplitude [kN]		34.6	4.3	47.8	4.6	43.4	18.1
	Maximum relative load within area of interest		1.049	1.095	1.050	1.092	1.051	1.104

4.1 Comparison

A comparison of the load distribution of the different test setups, as seen in Fig. ~~7~~8, shows that the solutions with springs ~~show~~ exhibit higher overloads outside the area of interest, where ~~it~~ this is permitted. This is due to the stiff springs which are attached outboard of the test area at 62% of the blade length to raise the eigenfrequency as much as possible. For the flapwise setup, this is seen in both uniaxial and biaxial tests. For the lead-lag direction, it is only seen for the uniaxial test, as the lead-lag eigenfrequency for the biaxial test had to be lowered to match the flapwise frequency. The overloaded area around 62% of the blade length would have to be further examined by the blade designer before testing in order to check if the design safety factors are high enough to withstand these loads. Otherwise, ~~It~~ consideration should be ~~considered~~ given to ~~reinforce~~ reinforcing ~~the overloaded area around 62%~~this part of the blade ~~length~~ in order to prevent damage~~s~~ and obviate the need for expensive repairs during testing. It ~~could~~ may also be possible to ~~distribute~~ spread the spring force ~~into~~ over two separate springs that are close to each other, but at different cross-sections. Using springs which are less stiff ~~springs~~ could also be a possibility, but would lead to lower frequencies and longer test times.

Kommentiert [MD22]: #14

The biaxial setup also exceeds the allowed lead-lag load by 0.4% at around 45% of the blade length, as the optimizer was unable to find a better solution. As this is still very close to the allowable range, the overload is considered to be acceptable. Overall, the test quality in terms of load distribution within the area of interest is similar and reasonable for all test setups.

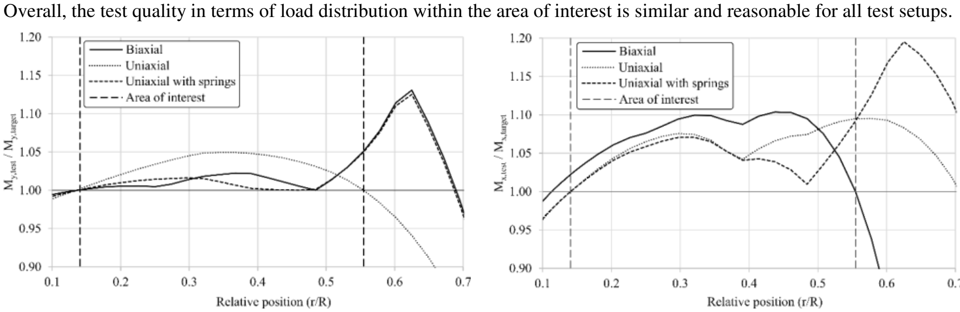

Figure 8~~7~~: Test load distribution relative to target load for different test setups in flapwise (left) and lead-lag (right) directions.

A comparison of the time required for the tests using the different setups is shown in Fig. ~~8~~9. The test times shown only take into account the active testing time; setup, inspections and trial runs are not considered. They are derived from the test frequency and the required number of cycles. The total time required by both consecutive uniaxial tests without springs is used as the baseline reference for the comparison, i.e. 100%. As the uniaxial lead-lag test needs twice as many cycles as the uniaxial flapwise test, it requires more time, even though the frequency is higher. When adding springs to the uniaxial tests, it is possible to reduce the total test time by 7%. Changing to biaxial tests can save an additional 24% of test time compared to the uniaxial test with springs.

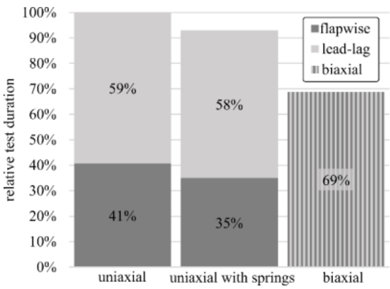

Figure 98: Relative comparison of test durations.

5 Summary and Outlook

~~In this~~This paper~~,~~ has presented an optimization scheme to find test setups for fatigue testing of wind turbine blades~~ was presented~~. Virtual masses and spring elements were implemented to tune the dynamic response of the test system. A case study was ~~done~~ undertaken on a representative blade. Results show that the ~~described~~ optimization method described is suitable to find both uniaxial and biaxial test setups.

For uniaxial test setups without spring elements, the optimization yielded results that satisfy all given boundary conditions in terms of required load distribution and local shear forces, yielding test frequencies of 0.57 Hz (flapwise) and 0.79 Hz (lead-lag direction). Compared to test setups that were defined manually, this is already an improvement in terms of testing time and overloading.

Furthermore, it was shown that an elliptical biaxial blade fatigue test using virtual masses and spring elements can save approximately 30% of testing time relative to consecutive state-of-the-art uniaxial fatigue tests.

As the results show, ~~particularly~~ for the flapwise test direction in particular, the required excitation forces are near the specified limit of 50 kN. This ~~occurs~~ is due to the high aerodynamic damping resulting from the flapwise motion. Combining the biaxial test with aerodynamic fairings, as proposed by Pan et al. (2017), may reduce the damping ~~may be reduced~~ and less force would then be needed.

Another approach to reduce the damping is to cut off more of the blade tip and combine biaxial with segmented testing. A further benefit of this would be the ~~mass~~ reduction in mass, thus raising natural frequencies and accelerating the test even further. In addition, the first flapwise and lead-lag natural frequencies of the root segment are closer to each other than those of the whole blade. ~~This way, less~~Thus, fewer virtual elements may be needed to ~~get~~ move the natural frequencies closer together to achieve elliptical biaxial testing.

Further future work includes extending the comparison of test loading and target loading in flapwise and lead-lag direction to off-axis directions.~~to off-axis load distribution of the test to the target loads, not only the flapwise and lead-lag loads.~~ This will show how much closer ~~the applied loads in biaxial testing are~~ to the field conditions the loading applied in biaxial testing is ~~as~~ compared to that in uniaxial tests.

Code/Data availability

The data that support~~s~~ the findings of this research are not publicly available due to confidentiality constraints.

Author contribution

DM, BM and SN conceptualized and defined the requirements for the method developed~~ method~~. BM supervised the work. DM developed the model code and performed the simulations. DM prepared the manuscript with contributions from all co-authors.

Competing interests

The authors declare that they have no conflict of interest.

Acknowledgements

We acknowledge the support within the Future Concept Fatigue Strength of Rotor Blades project granted by the German Federal Ministry for Economic Affairs and Energy (BMWi) (0325939) and the ~~The~~ Senator for Economic Affairs, Labour and Europe of the Free Hanseatic City of Bremen within the ERDF programme Bremen 2014-2020 (201/PF_IWES_ZK_Phase I/2017).

References

DNV GL AS: DNVGL-ST-0376 – Rotor blades for wind turbines, available at: https://rules.dnvgl.com/docs/pdf/DNVGL/ST/2015-12/DNVGL-ST-0376.pdf (last access: 07~~.~~ June 2019), 2015

Eder, M. A., Belloni, F., Tesauro, A., and Hanis, T.: A multi-frequency fatigue testing method for wind turbine rotor blades, J. Sound Vib., 388, 123–140, 2017.

Greaves, P. R., Dominy, R. G., Ingram, G. L., Long, H., and Court, R.: Evaluation of dual-axis fatigue testing of large wind turbine blades, P. I. Mech. Eng. C-J. Mec., 226, 1693–1704, 2012.

Greaves, P.R.: ORE Catapult Technical Note – Equivalent Drag Coefficients for ~~heaving~~ Heaving Airfoil, 2018.

Heijdra, J., Borst, M., and Van Delft, D.: Wind turbine blade structural performance testing, in: Advances in Wind Turbine Blade Design and ~~materials~~Materials, Woodhead Publishing, Sawston, Cambridge, UK, https://doi.org/10.1533/9780857097286.3.432, 432–445, 2013.

IEC: IEC 61400-23 – Wind Turbines Part 23: Full-scale structural testing of rotor blades, International Electrotechnical Commission, Geneva, Switzerland, 2014.

Lee, H. G. and Park, J.-S.: Optimization of resonance-type fatigue testing for a full-scale wind turbine blade, Wind Energy, 19, 371–380, 2016.

Pan, Z., Wu, J., Sun, Y. and Jian, L.: Effects of aerodynamic fairing on full scale blade fatigue test, IOP Conf. Series: Mat. Sc. and Eng., 207, 012083, 2017

Post, N., Bürkner, F.: Fatigue Test Design: Scenarios for Biaxial Fatigue Testing of a 60-Meter Wind Turbine Blade, Tech. rep., National Renewable Energy Laboratory, Golden, CO, USA, https://doi.org/10.2172/1271941, 2016.

Rosemeier, M., Basters, G. and Antoniou, A.: Benefits of subcomponent over full-scale blade testing elaborated on a trailing-edge bond line design validation, Wind Energy Science, 3, 163-172, doi:10.5194/wes-3-163-2018, 2018

Snowberg, D., Dana, S., Hughes, S., and Berling, P.: Implementation of a Biaxial Resonant Fatigue Test Method on a Large Wind Turbine Blade, Tech. rep., National Renewable Energy Laboratory, ~~National Renewable Energy Laboratory,~~ Golden, CO, USA, https://doi.org/10.2172/1155105, 2014.

White, D.: New method for dual-axis fatigue testing of large wind turbine blades using resonance excitation and spectral loading, Tech. rep., National Renewable Energy Lab., Golden, CO, USA, 2004.

White, D., Musial, W., and Engberg, S.: Evaluation of the new B-REX fatigue testing system for multi-megawatt wind turbine blades, in: Proceeding, ASME/AIAA Wind Energy Symposium, Reno, NV, 2005.

White, D., Desmond, M., Gowharji, W., Beckwith, J. A., and Meierjurgen, K.: Development of a dual-axis phase-locked resonant excitation test method for fatigue testing of wind turbine blades, in: ASME 2011 International Mechanical Engineering Congress & Exposition, 2011.

Zhang, J. Shi, K. and Liao, C.: Improved particle swarm optimization of designing resonance fatigue tests for large-scale wind turbine blades, J. of Renewable and Sustainable Energy, 10, 053303, doi: 10.1063/1.5018227, 2018